

# Algebraic analysis of electromagnetic chirality-induced negative refractive index in a four-level atomic system

Shuncaï Zhao <sup>1,\*</sup> Qi-Xuan Wu,<sup>2</sup> and Ai-Ling Gong<sup>1</sup>

<sup>1</sup>*Physics department, Kunming University of Science and Technology, Kunming, 650500, PR China*

<sup>2</sup>*College English department, Kunming University of Science and Technology, Kunming, 650500, PR China*

This paper presents a algebraic analysis of electromagnetic chirality-induced negative refractive index in a four-level atomic medium. According to analyze mathematically its argument of the complex refractive index for one circular polarization, it found that the negative refractive index without simultaneously negative permittivity and permeability can be obtained when the argument is in the second quadrant of the cartesian coordinate system, and that the probe field coupling to two equal transition frequencies in the atomic level doesn't require. This undoubtedly reduced stringent conditions to negative refractive index by quantum optics. As an application, our scheme may possibly give a novel approach to obtain negative refractive index by electromagnetic chirality-inducing.

arXiv:2402.09484v1 [quant-ph] 14 Feb 2024

---

\* Corresponding author: [zhaosc@kmust.edu.cn](mailto:zhaosc@kmust.edu.cn).

## I. INTRODUCTION

Negative refraction is an intriguing and counterintuitive phenomenon, and impressive efforts have recently been made to investigate negative refractive index materials[1]-[3]. Materials with negative refractive index promise many surprising properties: in the original description[4], it was stated that materials with negative refractive index promise many surprising and even counterintuitive electromagnetic and optical effects, such as the reversals of both Doppler shift and Cerenkov radiation[3], amplification of evanescent waves[5], subwavelength focusing[5]-[7] and so on. Up to now, there have been several approaches to the realization of negative refractive index materials, including artificial composite metamaterials[1],[8], photonic crystal structures[9], transmission line simulation[10] and chiral media[11]-[12] as well as photonic resonant materials (coherent atomic vapour)[13]-[18]. And the early proposals for negative refraction required media with both negative permittivity and permeability ( $\epsilon, \mu < 0$ ) in the frequency range of interest[4]. However, the typical magnetic dipole transition is smaller than electric dipole transition by a factor of the order of the fine structure constant ( $\alpha \approx \frac{1}{137}$ ). It is difficult to achieve negative permeability. An elegant scheme for negative refraction is proposed in the electromagnetic chirality medium without simultaneously negative permittivity and permeability[11],[19]-[22]. A medium in which the electric polarization  $\mathbf{P}$  is coupled to the magnetic field  $\mathbf{H}$  of an electromagnetic wave and the magnetization  $\mathbf{M}$  is coupled to the electric field  $\mathbf{E}$ [11]:

$$\mathbf{P} = \epsilon_0 \chi_e \mathbf{E} + \frac{\xi_{EH}}{c} \mathbf{H}, \mathbf{M} = \frac{\xi_{HE}}{c\mu_0} \mathbf{E} + \chi_m \mathbf{H}$$

Here  $\chi_e$  and  $\chi_m$ , and  $\xi_{EH}$  and  $\xi_{HE}$  are the electric and magnetic susceptibilities, and the complex chirality coefficients, respectively. They lead to additional contributions to the refractive index for one circular polarization[11],[20],[21]:

$$n = \sqrt{\epsilon\mu - \frac{(\xi_{EH} + \xi_{HE})^2}{4}} + \frac{i}{2}(\xi_{EH} - \xi_{HE}) \quad (1)$$

Obviously, if  $\xi_{EH} = -\xi_{HE} = i\xi$ , the real part of  $\sqrt{\epsilon\mu}$  is less than  $\xi$  ( $\xi > 0$ ), the negative refraction is obtained without requiring both  $\epsilon < 0$  and  $\mu < 0$ . In this paper, we analyze the argument of the complex number  $[\epsilon\mu - \frac{(\xi_{EH} + \xi_{HE})^2}{4}]$ , and get the conclusion that when its argument is in the second quadrant of the cartesian coordinate system, the argument of its square root  $[\sqrt{\epsilon\mu - \frac{(\xi_{EH} + \xi_{HE})^2}{4}}]$  has the possibility in the third quadrant accompanying with negative real part. Then the negative refractive index can be realized under the appropriate conditions without the stringent simultaneously negative permittivity and permeability.

The paper is organized as follows. In Section 2, we present our model and its expressions for the chirality coefficients and refractive index. In Section 3, we present numerical results and their discussion. This is followed by concluding remarks in Section 4.

## II. MODEL AND CHIRALITY COEFFICIENTS

In the following we mathematically analysis electromagnetically induced chiral negative refraction. The four-level configuration of atoms for consideration is shown in Figure 1. The parity properties of the atomic states are as following: levels  $|1\rangle$ ,  $|3\rangle$ , and  $|4\rangle$  have same parity, and level  $|2\rangle$  is opposite with theirs. Since the two lower levels  $|1\rangle$  and  $|2\rangle$  have opposite parity and so  $\langle 2|\hat{d}|1\rangle \neq 0$  where  $\hat{d}$  is the electric dipole operator. The two upper levels,  $|3\rangle$  and  $|4\rangle$  have the same parity with  $\langle 4|\hat{\mu}|3\rangle \neq 0$  where  $\hat{\mu}$  is the magnetic-dipole operator. As showed in Figure 1, three electromagnetic fields are introduced to couple the four states: The electric ( $\mathbf{E}$ ) and magnetic ( $\mathbf{B}$ ) components of the probe light (corresponding Rabi frequency  $\Omega_p = \frac{E_p d_{21}}{\hbar}$ ,  $\Omega_B = \frac{B_p \mu_{43}}{\hbar}$ ) interact with the transitions  $|2\rangle$  and  $|1\rangle$  as well as  $|4\rangle$  and  $|3\rangle$ , respectively. The incoherent pump field with pumping rate denoted by  $\Gamma$  pumps atoms in level  $|1\rangle$  into upper level  $|3\rangle$ , and then the atoms decay into metastable level  $|2\rangle$  via rapid nonradiative transitions, whose decay rate is denoted as  $\Gamma_{32}$ . The strong coherent field couples states  $|2\rangle$  and  $|4\rangle$  with Rabi frequency  $\Omega_c$ . The equation of

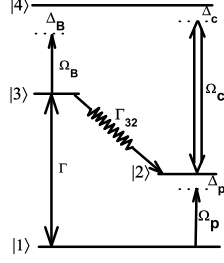


FIG. 1. Schematic diagram of a four-level atomic system interacting with a coherent  $\Omega_c$ , an incoherent pumps  $\Gamma$  and a probe field which electric and magnetic components are coupled to the level pairs  $|2\rangle - |1\rangle$  and  $|3\rangle - |4\rangle$ , respectively.

the time-evolution for the system is described as

$$\frac{d\rho}{dt} = -\frac{i}{\hbar}[H, \rho] + \Lambda\rho, \quad (2)$$

In which,  $\Lambda\rho$  represents the irreversible decay part in the system. Under the dipole approximation and the rotating wave approximation the density matrix equations described the system are written as follows:

$$\dot{\rho}_{11} = \Gamma(\rho_{33} - \rho_{11}) + \Gamma_{21}\rho_{22} + \Gamma_{31}\rho_{33} + \Gamma_{41}\rho_{44} + i\Omega_p(\rho_{21} - \rho_{12}), \quad (3)$$

$$\dot{\rho}_{21} = -(\gamma_{21} + i\Delta_p)\rho_{21} - i\Omega_p(\rho_{22} - \rho_{11}) + i\Omega_c\rho_{41}, \quad (4)$$

$$\dot{\rho}_{22} = -\Gamma_{21}\rho_{22} + \Gamma_{32}\rho_{32} + \Gamma_{42}\rho_{44} + i\Omega_p(\rho_{12} - \rho_{21}) + i\Omega_c(\rho_{42} - \rho_{24}), \quad (5)$$

$$\dot{\rho}_{31} = -[\gamma_{31} + i(\Delta_c + \delta)]\rho_{31} + i\Omega_p\rho_{32} + i\Omega_B\rho_{41}, \quad (6)$$

$$\dot{\rho}_{32} = -[\gamma_{32} + i(\Delta_c - \Delta_p + \delta)]\rho_{32} - i\Omega_c\rho_{34} - i\Omega_p\rho_{31} + i\Omega_B\rho_{42}, \quad (7)$$

$$\dot{\rho}_{33} = -\Gamma(\rho_{33} - \rho_{11}) - \Gamma_{31}\rho_{33} - \Gamma_{32}\rho_{33} + \Gamma_{43}\rho_{44} + i\Omega_B(\rho_{43} - \rho_{34}), \quad (8)$$

$$\dot{\rho}_{41} = -[\gamma_{41} + i(\Delta_p + \Delta_c)]\rho_{41} + i\Omega_c\rho_{21} - i\Omega_p\rho_{42} + i\Omega_B\rho_{31}, \quad (9)$$

$$\dot{\rho}_{42} = -(\gamma_{42} + i\Delta_c)\rho_{42} + i\Omega_c(\rho_{22} - \rho_{44}) - i\Omega_p\rho_{41} + i\Omega_B\rho_{32}, \quad (10)$$

$$\dot{\rho}_{43} = -[\gamma_{43} + i(\Delta_p - \delta)]\rho_{43} + i\Omega_c\rho_{23} + i\Omega_B(\rho_{33} - \rho_{44}) \quad (11)$$

where the above density matrix elements comply with the conditions:  $\rho_{11} + \rho_{22} + \rho_{33} + \rho_{44} = 1$  and  $\rho_{ij} = \rho_{ji}^*$ . And  $\Gamma_{ij}$  ( $i, j=1, 2, 3, 4$ ) is the spontaneous emission decay rate from level  $|i\rangle$  to level  $|j\rangle$ , ignoring the collision broaden effect.  $\gamma_{21} = \Gamma_{21}/2$ ,  $\gamma_{31} = (\Gamma_{31} + \Gamma_{32})/2$ ,  $\gamma_{41} = (\Gamma_{43} + \Gamma_{42})/2$ ,  $\gamma_{42} = (\Gamma_{43} + \Gamma_{31} + \Gamma_{21})/2$ ,  $\gamma_{43} = (\Gamma_{43} + \Gamma_{42} + \Gamma_{31} + \Gamma_{32})/2$ ,  $\gamma_{32} = (\Gamma_{32} + \Gamma_{31} + \Gamma_{21})/2$  are the decay rates to the corresponding transitions. The detuning of the fields defined as  $\Delta_p = \omega_{21} - \omega_p$ ,  $\Delta_c = \omega_{42} - \omega_c$ ,  $\Delta_B = \omega_{43} - \omega_p$ , respectively.  $\omega_{ij} = \omega_i - \omega_j$  is the transition frequency of level  $|i\rangle$  and  $|j\rangle$  ( $i, j=1, 2, 3, 4$ ) and we have  $\delta = \Delta_p - \Delta_B$ . Here we set  $\delta$  nonzero in order to avert the major obstacle mentioned in Ref.[16] in realizing the predicted effects at a realistic experimental setting. We solve for the steady-state values of the density matrix

elements  $\rho_{43}$  and  $\rho_{21}$  in a linear approximation when the probe field is weak, i.e.  $\Omega_p, \Omega_B \ll \Omega_c, \Gamma$ , and it can be assumed that almost all the atoms are in the ground state  $|1\rangle$ ,

$$\rho_{43} = a_1 \mathbf{E} + a_2 \mathbf{B}, \quad (12)$$

$$\rho_{21} = a_3 \mathbf{E} + a_4 \mathbf{B} \quad (13)$$

where the coefficients  $a_1, a_2$  and  $a_3, a_4$  are given by

$$a_1 = -\frac{d_{12}Z}{D_1 D_2^2 D_3 D_7 D_9 [(i\Delta_p + \gamma_{21})D_4 + \Omega_c^2] \hbar}, \quad (14)$$

$$a_2 = \frac{i\Gamma \mu_{34} \Omega_c^2}{D_1 D_2 D_3 D_9 \hbar}, \quad (15)$$

$$a_3 = \frac{i(D_4 + \frac{\Gamma \Omega_c^2}{D_1 D_9}) d_{12}}{[\Omega_c^2 + (\gamma_{21} - i\Delta_p) D_4] \hbar}, \quad (16)$$

$$a_4 = -\frac{\mu_{34} Z}{D_1 D_2 D_7 D_9 [(\gamma_{21} - i\Delta_p) D_4 + \Omega_c^2] \hbar} \quad (17)$$

and

$$Z = [D_1 D_2 \Gamma_{21} + i\Gamma(D_6 + D_8 - \gamma_{32} D_5)] \Omega_c^2, \quad (18)$$

$$D_1 = \gamma_{42} + i\Delta_c, D_2 = -i\gamma_{32} + \delta + \Delta_c - \Delta_p, \quad (19)$$

$$D_3 = i\gamma_{43} + \delta - \Delta_p, D_4 = \gamma_{41} + i(\Delta_c + \Delta_p), D_9 = \Gamma + \Gamma_{21}, \quad (20)$$

$$D_5 = \gamma_{42} + i(\Delta_c - \Delta_p), D_6 = i\gamma_{41} \Delta_p + i\gamma_{42} \Delta_p - \delta \Delta_p - 3\Delta_c \Delta_p + \Omega_c^2, \quad (21)$$

$$D_7 = -i\gamma_{31} + \delta + \Delta_c, D_8 = \gamma_{32} + \gamma_{41} + i(\delta + 2\Delta_c)(\Delta_c - i\gamma_{42})(\delta + \Delta_c) \quad (22)$$

The ensemble electric polarization and magnetization of the atomic medium to the probe field are given by  $\vec{P} = Nd_{12}\vec{\rho}_{21}$  and  $\vec{M} = N\vec{\mu}_{34}\rho_{43}$ , respectively, where  $N$  is the density of atoms. Then the coherent cross-coupling between electric and magnetic dipole transitions driven by the electric and magnetic components of the probe field may lead to chirality[11],[21]. Substituting equations (13) and (14) into the formula for the ensemble electric polarization and magnetization, we have the relations

$$\mathbf{P} = \alpha_{EE} \mathbf{E} + \alpha_{EB} \mathbf{B}, \mathbf{M} = \alpha_{BE} \mathbf{E} + \alpha_{BB} \mathbf{B}$$

where

$$\alpha_{EE} = Nd_{12}a_3, \alpha_{EB} = Nd_{12}a_4,$$

$$\alpha_{BE} = N\mu_{34}a_1, \alpha_{BB} = N\mu_{34}a_2$$

Considering both electric and magnetic local field effects[23]-[24],  $\mathbf{E}$  and  $\mathbf{B}$  in equation(24) must be replaced by the local fields

$$\mathbf{E}_L = \mathbf{E} + \frac{\mathbf{P}}{3\epsilon_0}, \mathbf{B}_L = \mu_0(\mathbf{H} + \frac{\mathbf{M}}{3})$$

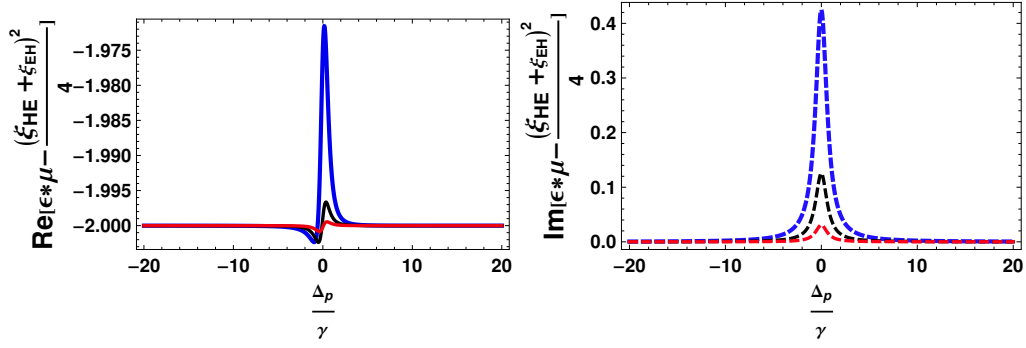


FIG. 2. The complex number  $[\varepsilon\mu - \frac{(\xi_{EH} + \xi_{HE})^2}{4}]$  as a function of the rescaled detuning parameter  $\Delta_p/\gamma$  for the three different sets of the pumping rate of the incoherent pump field and Rabi frequency of the coherent field ( $\Gamma, \Omega_c$ ), respectively.

As a result, we obtain

$$\mathbf{P} = \frac{3\varepsilon_0(\mu_0\alpha_{BB}\alpha_{EE} - \mu_0\alpha_{BE}\alpha_{EB} - 3\alpha_{EE})}{\mu_0\alpha_{BE}\alpha_{EB} + 3\alpha_{EE} - \mu_0\alpha_{BB}\alpha_{EE} - 9\varepsilon_0 + 3\mu_0\varepsilon_0\alpha_{BB}} \mathbf{E} + \frac{-9\mu_0\varepsilon_0\alpha_{EB}}{\mu_0\alpha_{BE}\alpha_{EB} + 3\alpha_{EE} - \mu_0\alpha_{BB}\alpha_{EE} - 9\varepsilon_0 + 3\mu_0\varepsilon_0\alpha_{BB}} \mathbf{H}, \quad (23)$$

$$\mathbf{M} = \frac{9\varepsilon_0\alpha_{BE}}{\mu_0\alpha_{BB}\alpha_{EE} + 9\varepsilon_0 - \mu_0\alpha_{BE}\alpha_{EB} - 3\alpha_{EE} - 3\varepsilon_0\mu_0\alpha_{BB}} \mathbf{E} + \frac{3(\mu_0\alpha_{BE}\alpha_{EB} - \mu_0\alpha_{BB}\alpha_{EE} + 3\varepsilon_0\mu_0\alpha_{BB})}{\mu_0\alpha_{BB}\alpha_{EE} + 9\varepsilon_0 - \mu_0\alpha_{BE}\alpha_{EB} - 3\alpha_{EE} - 3\varepsilon_0\mu_0\alpha_{BB}} \mathbf{H} \quad (24)$$

By comparison with equation (1), we obtain the permittivity and the permeability, and the complex chirality coefficients:

$$\varepsilon = 1 + \chi_e = \frac{6\alpha_{EE} + 9\varepsilon_0 + \mu_0[2\alpha_{BE}\alpha_{EB} - \alpha_{BB}(2\alpha_{EE} + 3\varepsilon_0)]}{-3\alpha_{EE} + \mu_0[-\alpha_{BE}\alpha_{EB} + \alpha_{BB}(\alpha_{EE} - 3\varepsilon_0)] + 9\varepsilon_0}, \quad (25)$$

$$\mu = 1 + \chi_m = \frac{-3\alpha_{EE} + 2\mu_0[\alpha_{BE}\alpha_{EB} - \alpha_{BB}(\alpha_{EE} - 3\varepsilon_0)] + 9\varepsilon_0}{-3\alpha_{EE} + \mu_0[-\alpha_{BE}\alpha_{EB} + \alpha_{BB}(\alpha_{EE} - 3\varepsilon_0)] + 9\varepsilon_0}, \quad (26)$$

$$\xi_{EH} = \frac{9c\mu_0\alpha_{EB}\varepsilon_0}{-3\alpha_{EE} + \mu_0[-\alpha_{BE}\alpha_{EB} + \alpha_{BB}(\alpha_{EE} - 3\varepsilon_0)] + 9\varepsilon_0}, \quad (27)$$

$$\xi_{HE} = \frac{9c\mu_0\alpha_{BE}\varepsilon_0}{-3\alpha_{EE} + \mu_0[-\alpha_{BE}\alpha_{EB} + \alpha_{BB}(\alpha_{EE} - 3\varepsilon_0)] + 9\varepsilon_0} \quad (28)$$

In the above, we obtained the expressions for the electric permittivity and magnetic permeability of the atomic media. Substituting equations from (30) to (33) into (2), the expression for refractive index can also be presented. In the section that follows, we will discuss the negative refractive index of the atomic system without requiring simultaneously negative both permittivity and permeability under the appropriate conditions.

### III. RESULTS AND DISCUSSIONS

Before doing these calculations, we need to fix several key parameters such as spontaneous emission rate, wavelength and atomic density in these equations. In the model configuration, the transition from  $|4\rangle$  to  $|3\rangle$  is magnetic dipole allowed

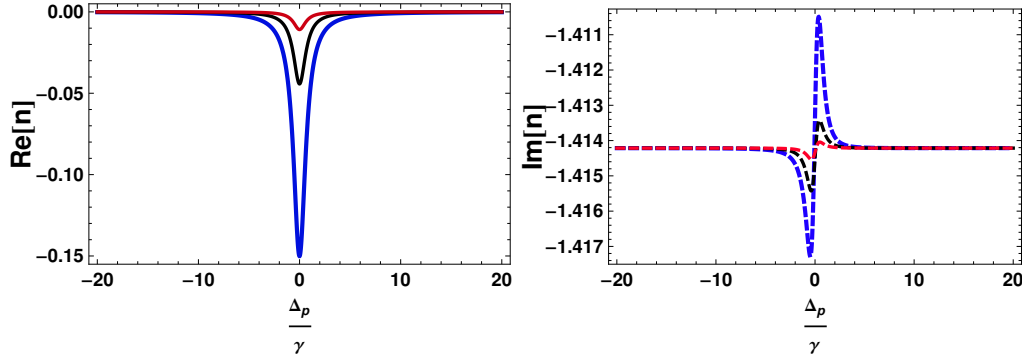


FIG. 3. The real and imaginary parts of the refractive index as a function of the rescaled detuning parameter  $\Delta_p/\gamma$  for the three different sets of pumping rate of the incoherent pump field and Rabi frequency of the coherent field ( $\Gamma, \Omega_c$ ), respectively.

and others are electrical dipole allowed. The typical value of the spontaneous emission rate of atomic electric dipole transitions is the magnitude of  $10^8$  Hz. The spontaneous emission rate of atomic magnetic dipole transitions is in general smaller than that of atomic electric dipole transitions by four magnitude. Thus, in our numerical calculations, the spontaneous emission rates are scaled by  $\gamma = 10^8 s^{-1}$ :  $\Gamma_{43} = \Gamma_{21} \times (\frac{1}{137})^2$ ,  $\Gamma_{21} = 1\gamma$ ,  $\Gamma_{41} = 0.1\gamma$ ,  $\Gamma_{42} = 0.9\gamma$ ,  $\Gamma_{31} = 0.3\gamma$ ,  $\Gamma_{32} = 0.2\gamma$ . The typical optical wavelength for the transitions  $|4\rangle \rightarrow |3\rangle$  and  $|2\rangle \rightarrow |1\rangle$  is selected to be 600 nm[22,23]. The dipole moments  $d_{12}$  and  $\mu_{34}$  are estimated by the relation  $\sqrt{3\hbar\Gamma_{ij}\lambda^3/8\pi^2}$ . In the present calculations, we choose the density of atoms  $N$  to be  $5 \times 10^{22} m^{-3}$ . The level configuration shown in figure 1 may be realized in the trivalent positive ions  $E_r^{3+}$  doped into calcium fluorophosphate at room temperature, which has abundant energy levels, various electric magnetic transitions and high density[27],[28]. The four levels  $|1\rangle, |2\rangle, |3\rangle$ , and  $|4\rangle$  in Figure 1 may correspond to the energy level configuration  $I_{15/2}^4, I_{13/2}^4, I_{9/2}^4$  and  $I_{11/2}^4$  of the rare earth ion  $E_r^{3+}$  doped in calcium fluorophosphate, respectively. The detuning of the strong coherent field is set as  $-5 \times 10^{-3}\gamma$ , and the difference of electric and magnetic coupling  $\delta = -10^{-3}\gamma$ . In Ref.[16], the probe field hypothesized resonance with the electric and magnetic transitions is considered a major obstacle in realizing the predicted effects at a realistic experimental setting, as it is not straightforward to find a system with two states fitting the condition. And in our scheme the obstacle dissolve because the electric and magnetic transitions are set to be off-resonant.

The pumping rate of the incoherent pump field  $\Gamma$  and the Rabi frequency of the coherent field  $\Omega_c$  are set as parameter group  $(\Gamma, \Omega_c)$  in the following discussion. And the blue, black and red curves in all the figures are corresponding to the three different parameter groups,  $(5\gamma, 20\gamma)$ ,  $(50\gamma, 10\gamma)$  and  $(25\gamma, 5\gamma)$ , respectively. In figure 2, the complex number  $[\varepsilon\mu - \frac{(\xi_{EH} + \xi_{HE})^2}{4}]$  is shown against the rescaled detuning parameter  $\Delta_p/\gamma$ . It is observed that the sign of the real parts of the complex number is minus with the different parameter groups, while its imaginary part remains positive sign when the parameter groups vary with the three different values. At the resonant point the peak values are decreasing with the diminish of the Rabi frequency  $\Omega_c$ . With regard to a complex number, its argument is in the second quadrant of cartesian coordinates system when it has minus real part and positive imaginary part. And the principal argument value of the square root  $[\sqrt{\varepsilon\mu - \frac{(\xi_{EH} + \xi_{HE})^2}{4}}]$  is a half of the complex number  $[\varepsilon\mu - \frac{(\xi_{EH} + \xi_{HE})^2}{4}]$ . Because the argument of  $[\sqrt{\varepsilon\mu - \frac{(\xi_{EH} + \xi_{HE})^2}{4}}]$  is constituted by the principal argument angle and  $k\pi$ , its phase is in the third quadrant of cartesian coordinates when  $k$  is assigned to an odd number. Thus the real part of the first part of the refractive index gets negative value, because its first part is  $[\sqrt{\varepsilon\mu - \frac{(\xi_{EH} + \xi_{HE})^2}{4}}]$ . In equation(2), the real part of the refractive index gets negative value if its first part has sufficiently large magnitude.

In figure 3, the refraction index is plotted for the different three parameter groups. It's observed that the real and imaginary parts of the refractive index are negative and their the largest absolute value present to the resonant point when  $\Omega_c = 20\gamma$ . In figure 4, the permittivity is shown against the rescaled detuning parameter  $\Delta_p/\gamma$ . As shown in figure 4, the rescaled real parts of permittivity  $(Re[\varepsilon] - 1)$  have the same order of magnitude  $10^{-13}$ , and the same value

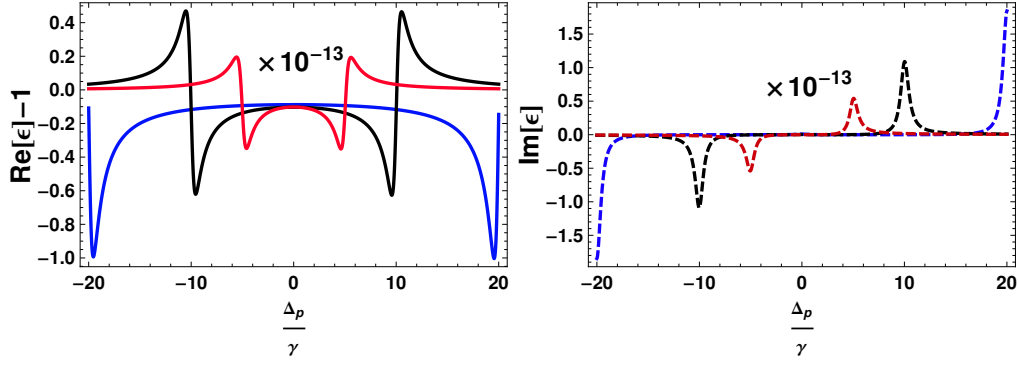


FIG. 4. The real and imaginary parts of the permittivity as a function of the rescaled detuning parameter  $\Delta_p/\gamma$  for the three different sets of pumping rate of the incoherent pump field and Rabi frequency of the coherent field ( $\Gamma, \Omega_c$ ), respectively.

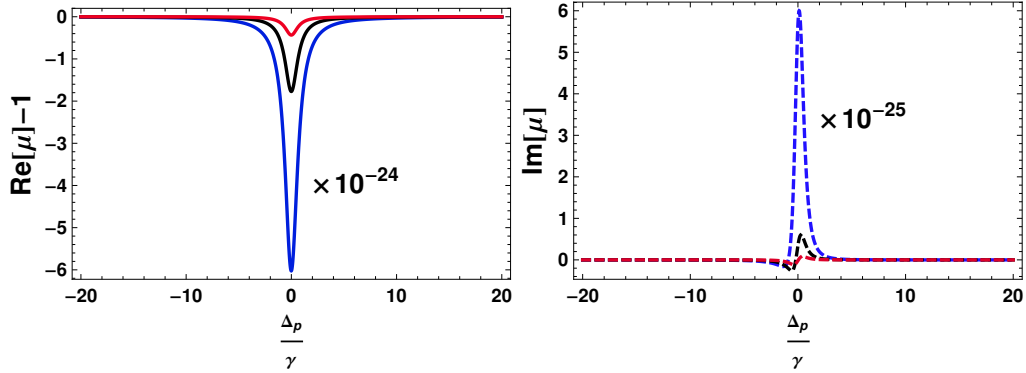


FIG. 5. The real and imaginary parts of the permeability as a function of the rescaled detuning parameter  $\Delta_p/\gamma$  for the three different sets of pumping rate of the incoherent pump field and Rabi frequency of the coherent field ( $\Gamma, \Omega_c$ ), respectively.

$-0.1$  in the near of magnitude ( $10^{-13}$ ) is far less than the number 1. We note that the imaginary part of permittivity has the same order of magnitude with its real part. Beside the absorption peaks and the gain vales at the symmetry points, the transparent windows appear in the curves of the imaginary part of permittivity. Which concludes that the maximum intensity of the coherent field produces the widest transparent window. From the figure 5, we observed the rescaled real part permeability ( $Re[\mu] - 1$ ) has a more less order of magnitude ( $10^{-24}$ ) than that of the rescaled real parts of permittivity ( $Re[\varepsilon] - 1$ ). And the imaginary part  $Im[\mu]$  gets the magnitude of ( $10^{-25}$ ). As shown in figure 5, the response from the external fields only concentrates in the near resonant region. And the strongest coherent field corresponds the largest permeability. The magnitude of the rescaled real parts of permittivity ( $Re[\mu] - 1$ ) is  $Re[\mu] \approx 1$ . Thus the electric and magnetic susceptibilities are weak because of  $Re[\varepsilon] \approx 1$  and  $Re[\mu] \approx 1$ . So we obtain the negative refraction completely resulted from the electromagnetically induced chirality in the scheme.

#### IV. CONCLUSION

In summary, electromagnetic chirality-induced negative refraction in a four-level atomic medium is obtained by the algebraic analysis to the argument of the refractive index for one circular polarization. When two unequal transition frequencies responding to the electric and magnetic transitions of the probe field and the parameter groups ( $\Gamma, \Omega_c$ ) getting different values, the atomic system shows negative refraction without requiring both electric permittivity and magnetic permeability to be simultaneously negative. Compared with the method of realizing negative fraction[20],[25], our algebraic analysis scheme seems to reduce the difficulty and provide more possibilities. It may possibly give a

novel approach to obtain the desired material with negative refractive index by electromagnetic chirality-inducing.

- 
- [1] R. Shelby, D. R. Smith, and S. Schultz, *Science* **292** 77 (2001).
- [2] T. J. Yen, W. J. Padilla, et al. *Science***303** 1494(2004).
- [3] V. G. Veselago, E. E. Narimanov, *Nature Mater.* **5** 759(2006).
- [4] V. G. Veselago, *Soviet Physics Usp.* **10** 509(1968).
- [5] J. B. Pendry, *Phys.Rev.Lett.* **85** 3966(2000).
- [6] K. Aydin, I. Bulu and E. Ozbay, *Appl. Phys. Lett.* **90** 254102(2007).
- [7] L. Chen, S. He, L. Shen, *Phys. Rev. Lett.* **92** 107404(2004).
- [8] J. B. Pendry, *Nature* **423** 22-23 (2003).
- [9] E. Cubukcu, K. Aydin, E. Ozbay, S. Foteinopoulou, and C. M. Soukoulis, *Nature* **423** 604(2003).
- [10] G. V. Eleftheriades, A. K. Iyer, P. C. Kremer, *IEEE Trans. Microwave Theory Tech.* **50** 2702(2002).
- [11] J. B. Pendry, *Science* **306**1353(2004).
- [12] V. Yannopapas, *J.Phys.:Condens.Matter* **18**6883(2006).
- [13] S. C. Zhao, *JETP Lett.***94** 347-352(2011).
- [14] Q. Thommen, P. Mandel, *Phys. Rev. Lett.* **96** 053601 (2006).
- [15] S. C. Zhao, Z. D. Liu, J. Zheng, G. Li, N. Liu, *Optik* **123** 1063 (2012).
- [16] M. Ö. Oktel, Ö. E. Müteçaplıoğlu, *Phys. Rev. A* **70** 053806 (2004).
- [17] S. C. Zhao, *Sci China-Phys Mech Astron* **55** 213(2012).
- [18] J. Q. Shen, *Phys. Lett. A* **357** 54(2006).
- [19] C. Monzon and D. W. Forester, *Phys. Rev. Lett.* **95**123904 (2005).
- [20] J. Kästel, M. Fleischhauer, S. F. Yelin and R. L. Walsworth, *Phys. Rev. Lett.* **99** 073602 (2007).
- [21] J. Kästel, M. Fleischhauer, R. L. Walsworth, *Phys. Rev. A* **79** 063818 (2009).
- [22] T. G. Mackay, A. Lakhtakia, [[http:// dx. doi. org/ 10. 1117/6. 0000003](http://dx.doi.org/10.1117/6.0000003)].
- [23] D. M. Cook *The Theory of the Electromagnetic Field*, Prentice-Hall, New Jersey **chapter 11** (1975).
- [24] J. D. Jackson, *Classical Electrodynamics(3rd edn)*, New York: Wiley **p160** (1999 ).
- [25] F. L. Li, A. P. Fang, M. Wang, *J. Phys. B***42**199505(2009).
- [26] H. J. Zhang, Y. P. Niu, H. Sun, J. Luo and S. Q. Gong, *J. Phys. B***41**125503(2008).
- [27] A. A. Kaminskii, V. Mironov, S. A. Kornienko, S. N. Bagaev, G. Boulon, A. Brenier, B. DiBartolo, *Phys. Status Solidi A* **151** 231 (1995).
- [28] D. K. Sardar, C. H. Coeckelenbergh, R. M. Yow, J. B. Gruber, T. H. Allik, *J. Appl. Phys.***98** 033535 (2005).